Computer-aided Diagnosis of Retinopathy of Prematurity

Rangaraj M. Rangayyan,

Faraz Oloumi, and Anna L. Ells

Department of Electrical and Computer Engineering, University of Calgary

Alberta Children's Hospital, Division of Ophthalmology, Department of Surgery

Calgary, Alberta, Canada

UNIVERSITY OF CALGARY

UNIVERSITY OF CALGARY

Imaging of the Fundus of the Retina

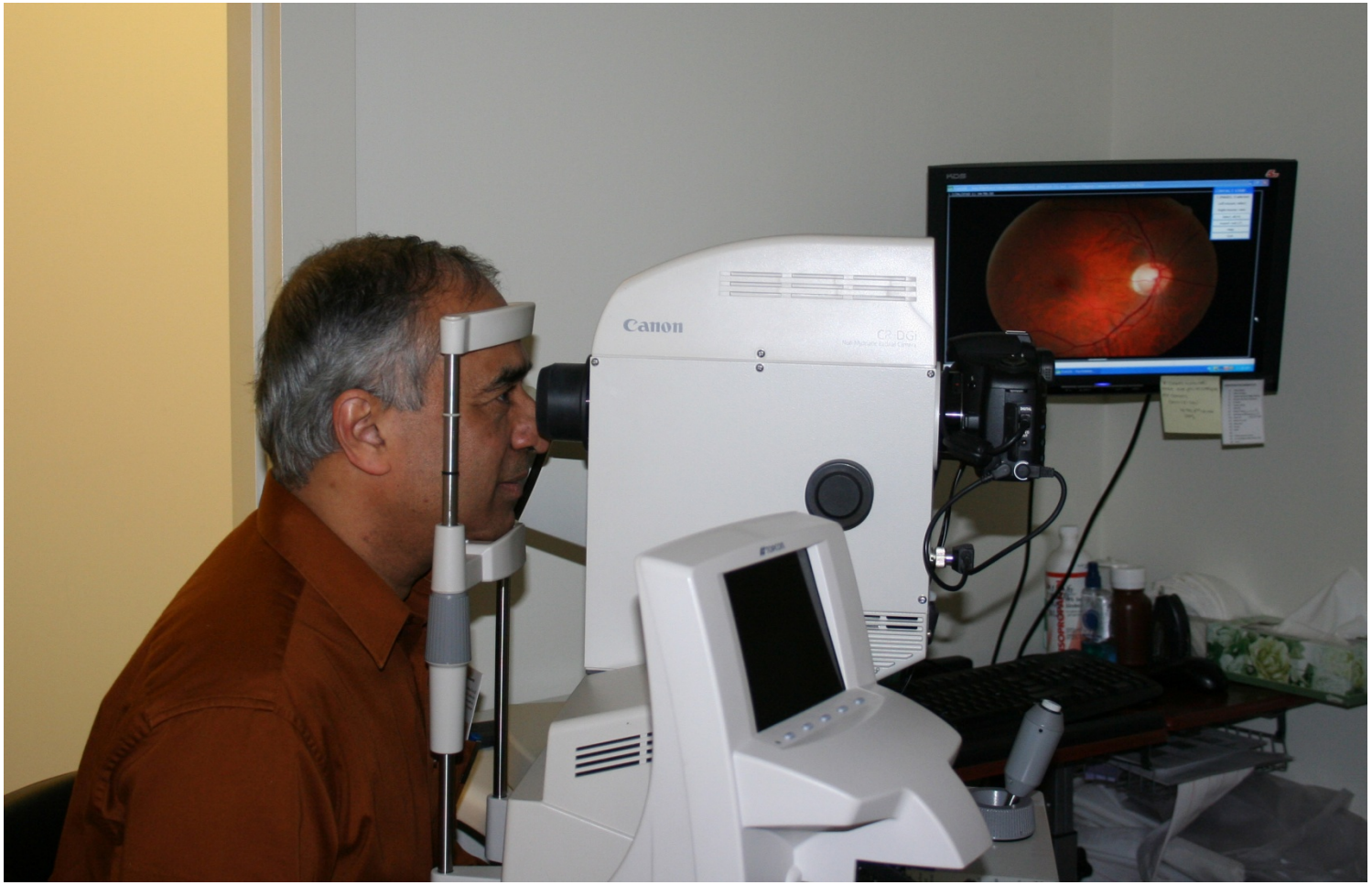

UNIVERSITY OF CALGARY

Retinopathy of Prematurity

- Retinopathy of prematurity (RoP) can develop in the first 8 to 12 weeks of life
- RoP is a leading cause of preventable childhood blindness
- Risk factors: birth weight < 1250 to 1750 *g* and gestational age < 28 to 32 weeks

Image Alert!

Imaging of the Retinal Fundus of Premature Infants with the RetCam

1. Topical anesthesia / speculum

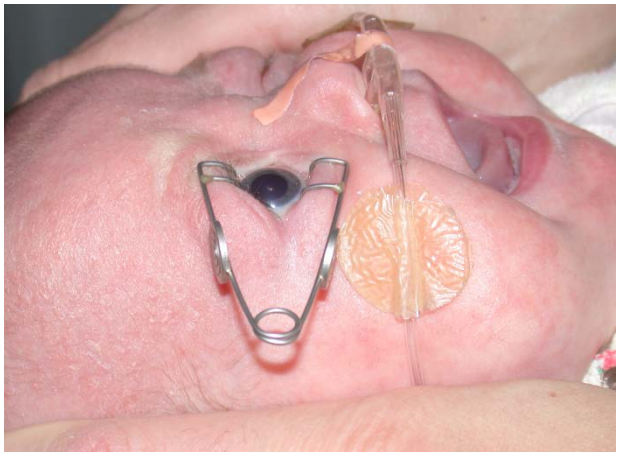

2. Coupling gel to tip

3. Application of camera tip

4. Image capture

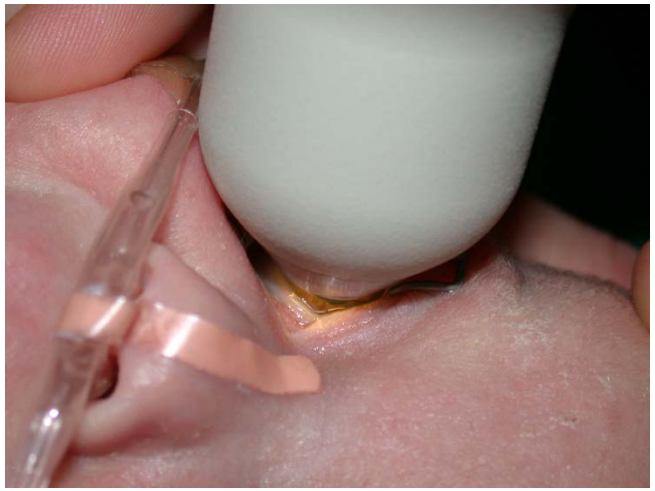

UNIVERSITY OF CALGARY

Stages of RoP

RoP 0

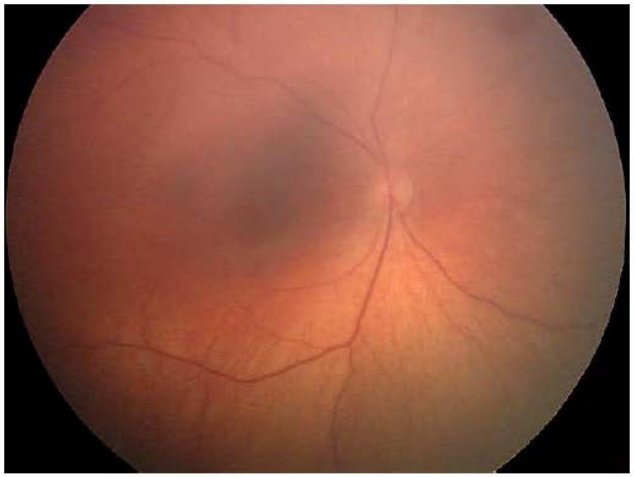

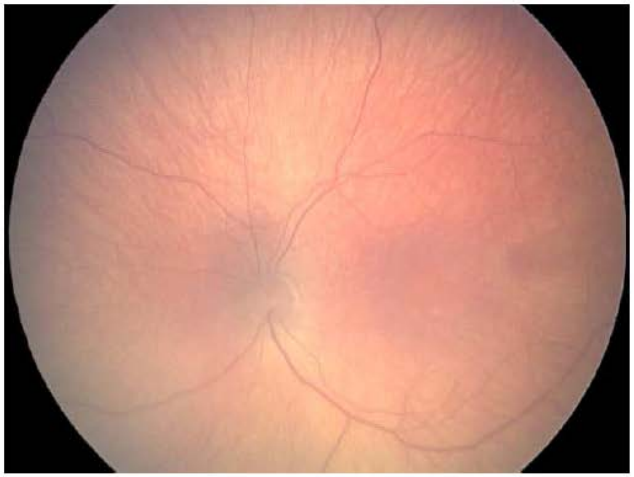

RoP 1

RoP 2

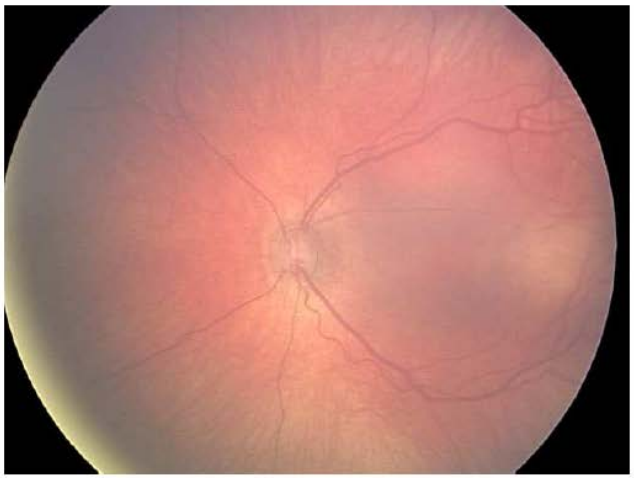

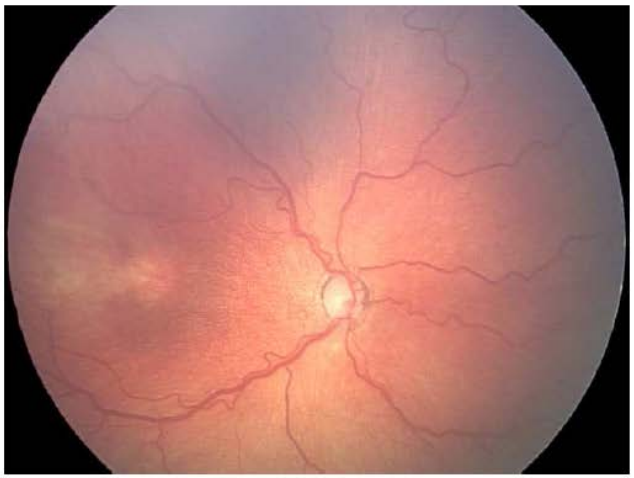

RoP 3

UNIVERSITY OF CALGARY

Indicators of Severity of RoP

- Previously assessed solely based on abnormal vascular response
- Recently established: early treatment should be based on the presence of plus disease
- Vascular signs of plus disease are
  - Increased dilation and tortuosity
  - Straightening of the major temporal arcade (MTA)

UNIVERSITY OF CALGARY

Plus Disease

- Diagnosed by a certain level of increase in dilation and tortuosity of vessels
- Clinical diagnosis performed by visual qualitative comparison to a gold-standard retinal fundus image
- Considered to be the main indicator for early diagnosis and treatment of RoP

UNIVERSITY OF CALGARY

Example of Plus Disease

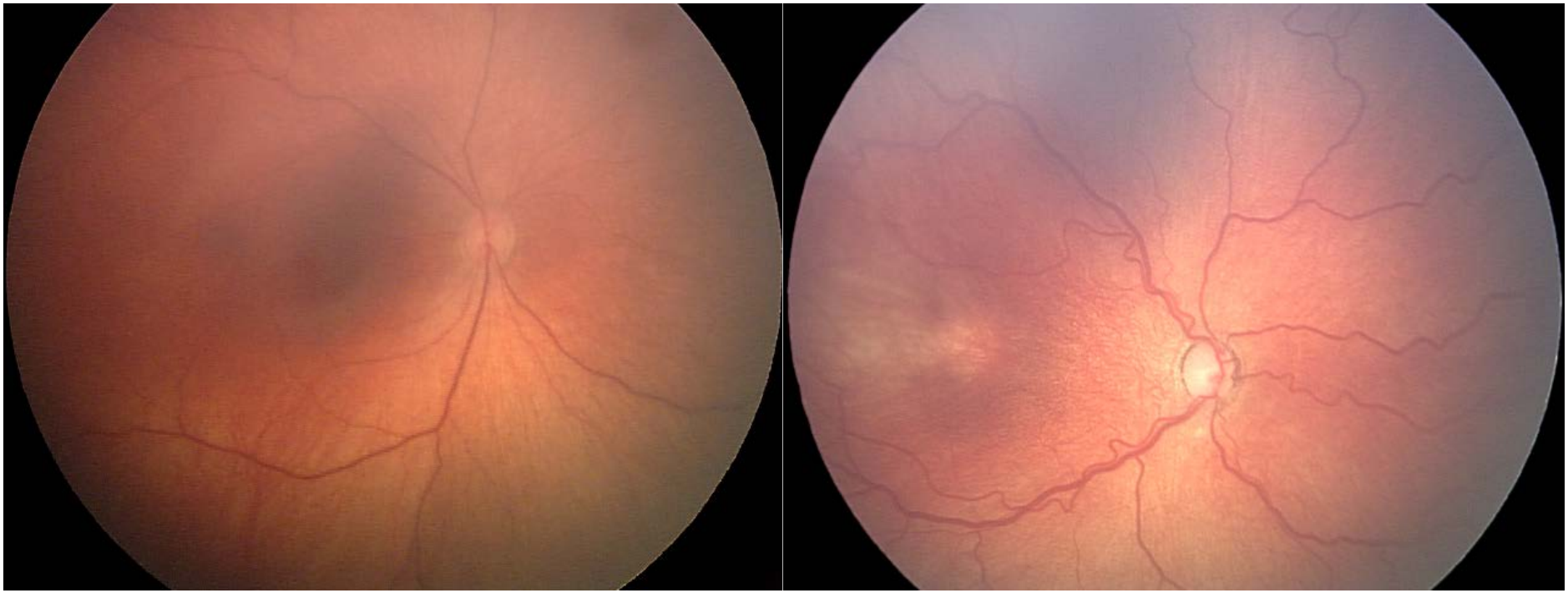

No RoP

RoP with plus disease

UNIVERSITY OF CALGARY

Objectives of our Study

- Detection of the MTA and measurement of its thickness
- Quantification of the openness of the MTA via parabolic modeling and by measurement of the temporal arcade angle (TAA)
- Quantification of vascular tortuosity
- Computer-aided diagnosis (CAD) of RoP

UNIVERSITY OF CALGARY

Telemedicine for RoP In Calgary Database

- Methods tested with retinal fundus images from the Telemedicine for RoP In Calgary (TROPIC) database
- Images captured using wide-field (130°) RetCam 130 camera (640 × 480 pixels)
- Spatial resolution estimated to be 30 μm/pixel
- Nineteen images associated with plus disease and 91 showing no signs of plus disease

UNIVERSITY OF CALGARY

Statistics of the TROPIC Database

Parameter	No Plus Disease Mean ± STD ($n = 91$)	Plus, Mean ± STD ($n = 19$)
BW (g)	818.00 ± 210.78	815.89 ± 203.71
GA (weeks)	26.73 ± 1.88	24.95 ± 1.77
CA (days)	71.05 ± 23.67	69.84 ± 13.00

BW: Birth weight; GA: Gestational age; CA: Chronological age;

n = number of images; number of patients = 41

UNIVERSITY OF CALGARY

DRIVE Database of Retinal Images

- The Digital Retinal Images for Vessel Extraction (DRIVE) database (40 images) used for testing algorithms
- Image size 584 x 565 pixels (20 μm/pixel)
- The MTAs were traced by a pediatric ophthalmologist and retina specialist (Dr. Ells)
- The hand-drawn traces of the MTA were used for evaluation of the tracking algorithm

UNIVERSITY OF CALGARY

Anatomical Features of the Retina

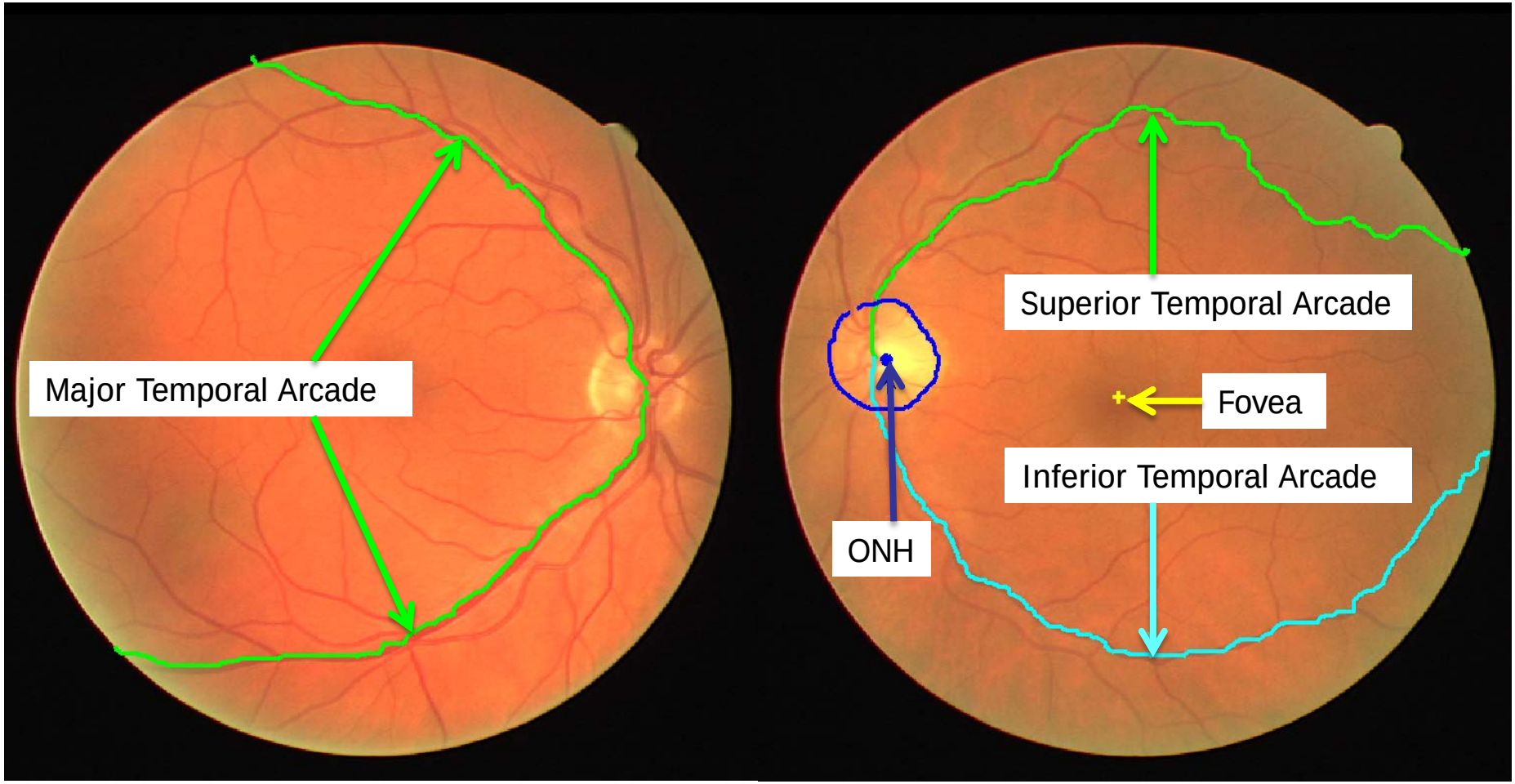

ONH: Optic Nerve Head

UNIVERSITY OF CALGARY

Detection of Vessels: Gabor Filters

Gabor filters are sinusoidally modulated Gaussians: *provide optimal localization in both the frequency and space domains*

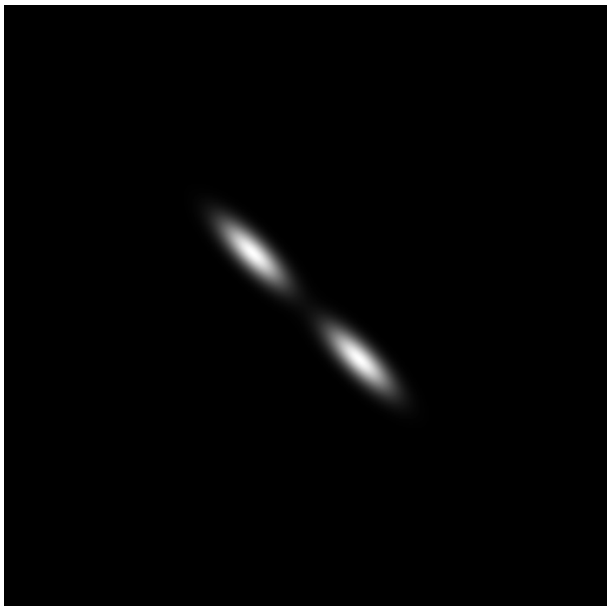

UNIVERSITY OF CALGARY

Design of Gabor Filters as Line Detectors

$$g(x,y)=\frac{1}{2\pi\sigma_x\sigma_y}\exp\left[-\frac{1}{2}\left(\frac{x^2}{\sigma_x^2}+\frac{y^2}{\sigma_y^2}\right)\right]\cos(2\pi f x)$$

Design parameters

- line thickness τ
- elongation l
- orientation θ

Gabor parameters

$$f=\frac{1}{\tau};\qquad \sigma_x=\frac{\tau}{2\sqrt{2\ln 2}}$$

$$\sigma_y=l\sigma_x;\qquad \begin{bmatrix}x\\y\end{bmatrix}=\begin{bmatrix}\cos\theta & -\sin\theta\\ \sin\theta & \cos\theta\end{bmatrix}\begin{bmatrix}x'\\y'\end{bmatrix}$$

Gabor Filters: Impulse Response and Frequency Response

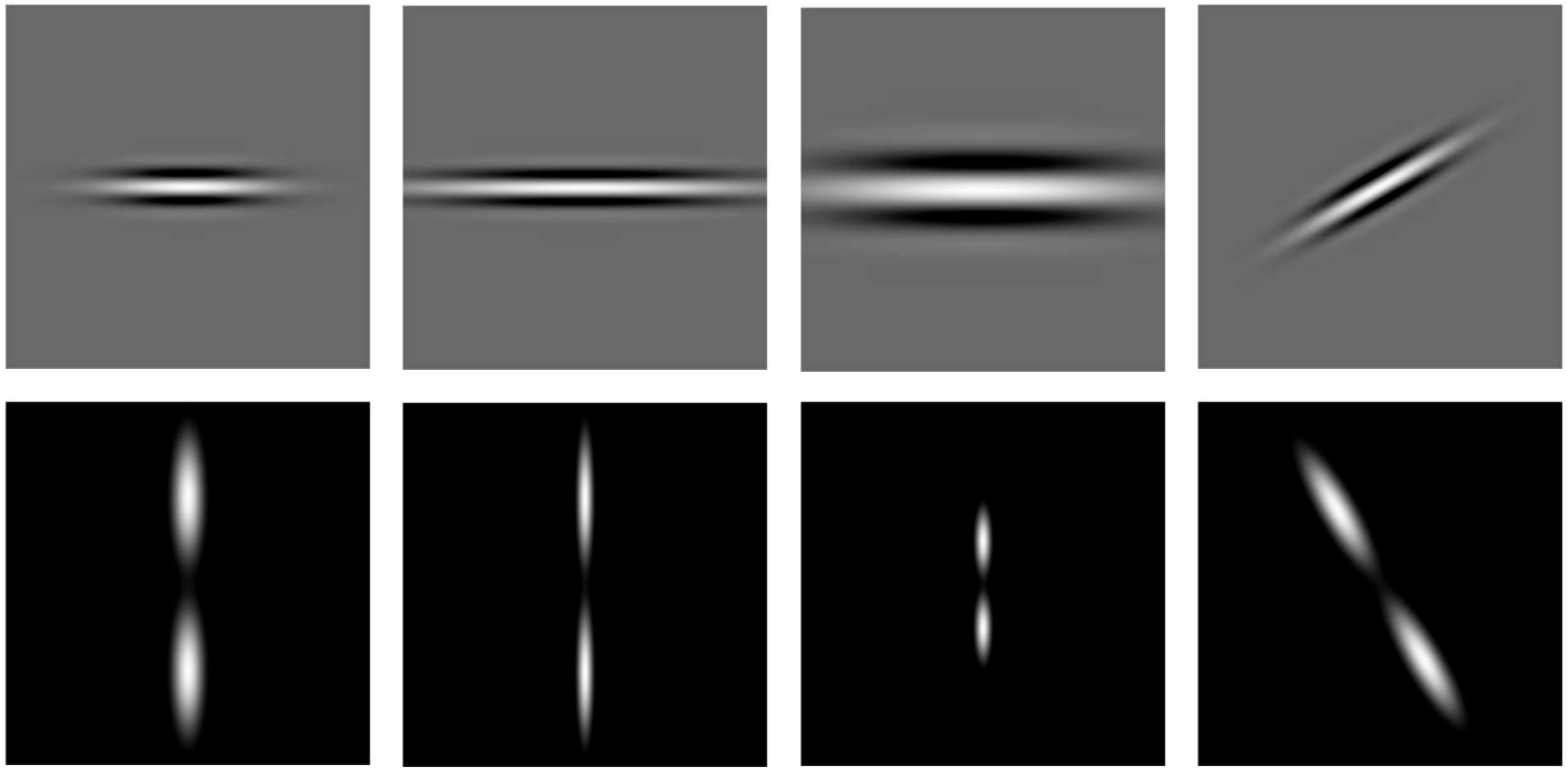

$l = l_0$	$l > l_0$	$l = l_0$	$l = l_0$
$\tau = \tau_0$	$\tau = \tau_0$	$\tau > \tau_0$	$\tau = \tau_0$
$\theta = \theta_0$	$\theta = \theta_0$	$\theta = \theta_0$	$\theta > \theta_0$

UNIVERSITY OF CALGARY

Results of Gabor Filtering

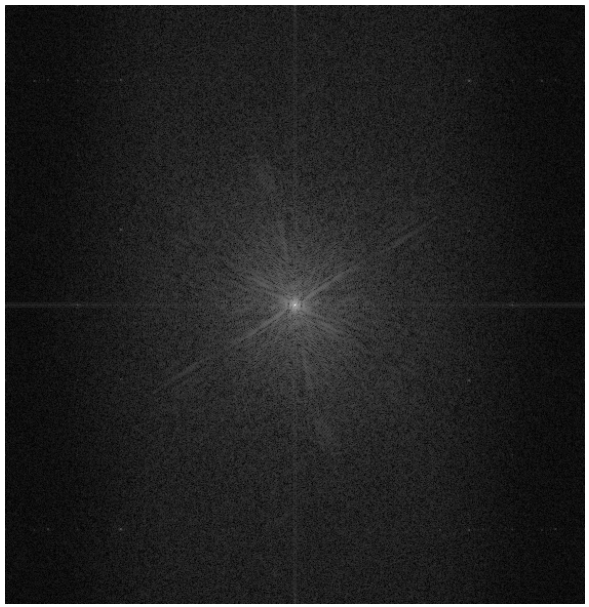

Log magnitude spectrum

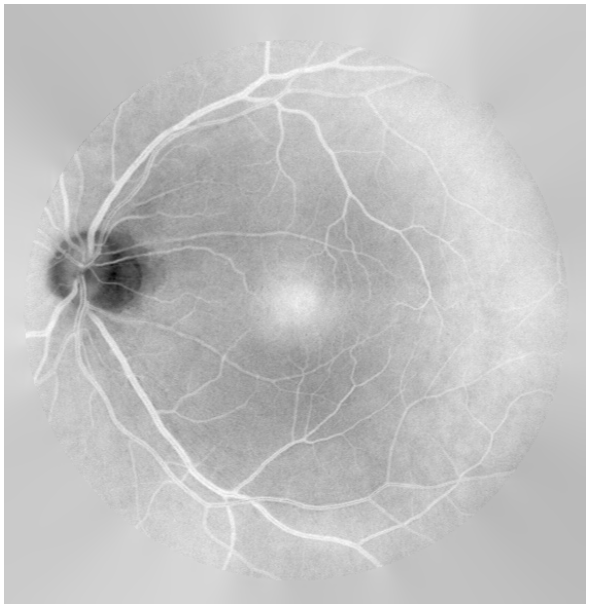

Inverted Y channel

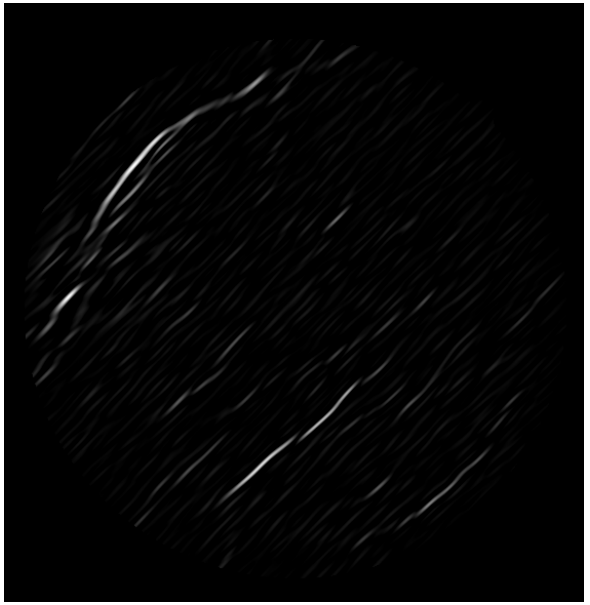

Magnitude response of a single Gabor filter:

$\tau = 8,\ l = 2.9, \theta = 45^{o}$

UNIVERSITY OF CALGARY

Detection of Blood Vessels

- Bank of 180 real Gabor filters spaced evenly over [-90^o, 90^o] with elongation l = 1 and thickness τ = 7 pixels used

- Gabor magnitude response (GMR) at each pixel = max filter response over all angles

- Vessel orientation at each pixel $\phi(p)$ = orientation of filter with max response

UNIVERSITY OF CALGARY

Results of Gabor Filtering

Orientation field

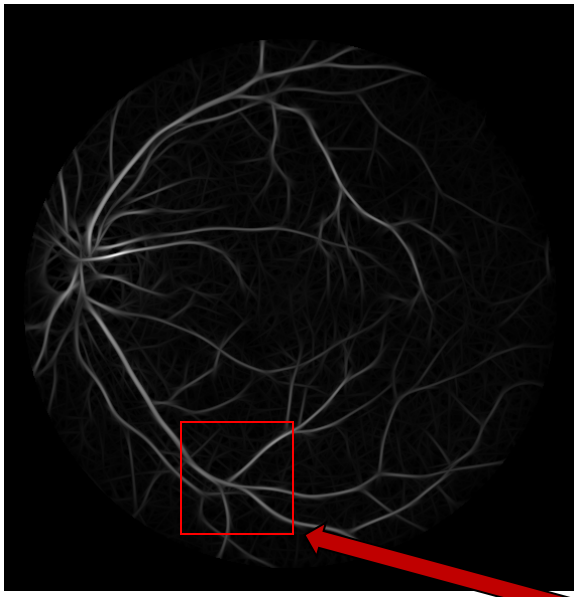

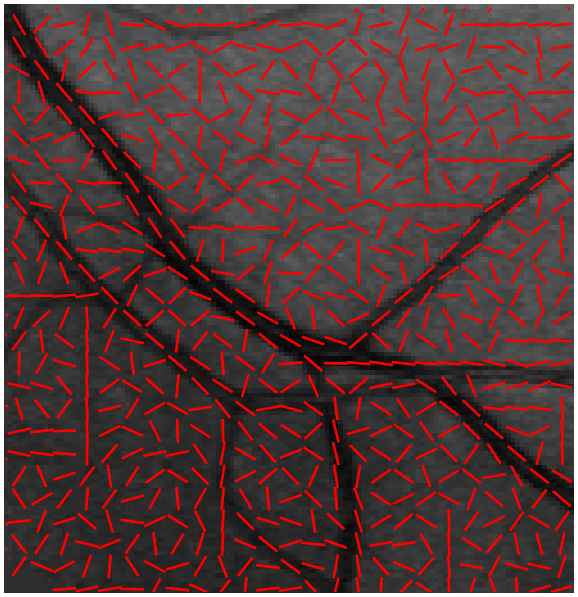

Original image

Gabor magnitude (max over 180 angles)

Gabor angle (zoomed)

UNIVERSITY OF CALGARY

Comparative Analysis with Other Works

Detection method	A_z
Matched filter; Chaudhuri et al.	0.91
Adaptive local thresholding; Jiang and Mojon	0.93
Ridge-based segmentation; Staal et al.	0.95
Single-scale Gabor filters; Rangayyan et al.	0.95
Multiscale Gabor filters; Soares et al.	0.96
Multiscale Gabor filters; present work	0.96

Area under the receiver operating characteristic (ROC) curve (A_z) with 20 test images from DRIVE

UNIVERSITY OF CALGARY

Detection of the ONH: Convergence of Blood Vessels

1. Extract the orientation field using Gabor filters
2. Filter and down-sample the orientation field
3. Analyze the orientation field using phase portraits
4. Postprocess the phase portrait maps
5. Detect sites of convergence of blood vessels
6. Select the point of convergence to represent the center of the ONH

UNIVERSITY OF CALGARY

Phase Portraits

$$\vec{\mathbf{v}}(x,y) = \begin{pmatrix} v_x \\ v_y \end{pmatrix} = \mathbf{A}\begin{pmatrix} x \\ y \end{pmatrix} + \mathbf{b}, \qquad \mathbf{A} = \begin{bmatrix} a & b \\ b & c \end{bmatrix}, \ \mathbf{b} = \begin{bmatrix} d \\ e \end{bmatrix}$$

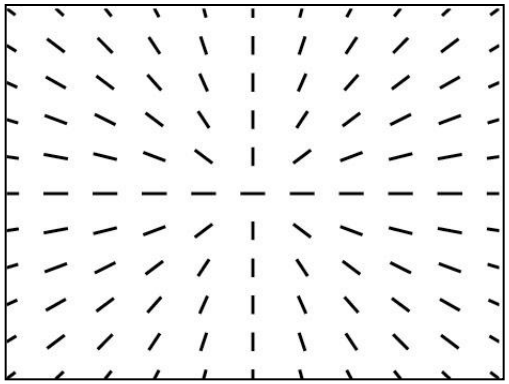

node

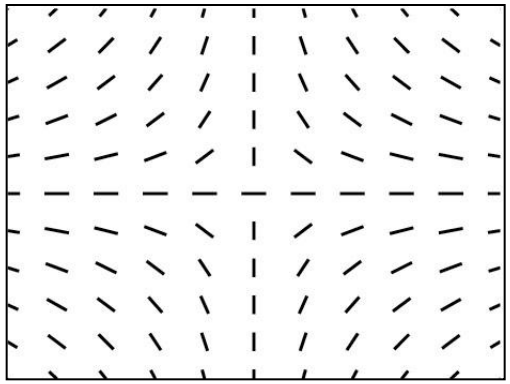

saddle

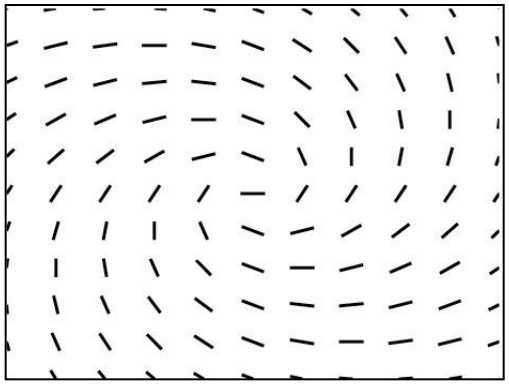

(spiral)

UNIVERSITY OF CALGARY

Phase Portrait Analysis

Fit phase portrait model to the analysis window

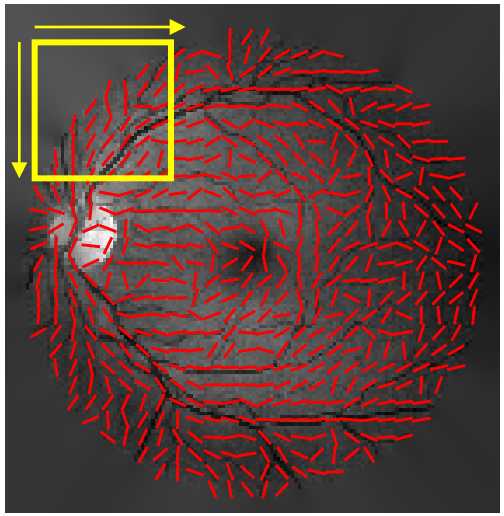

Window size:
40 × 40 pixels

$$\mathbf{A} = \begin{bmatrix} 1.1 & 0.3 \\ 0.3 & 1.7 \end{bmatrix}$$

$$\mathbf{b} = \begin{bmatrix} -4.8 \\ -7.9 \end{bmatrix}$$

Phase Portrait Analysis

Cast a vote at the fixed point given by $-\mathbf{A}^{-1}\mathbf{b}$

in the corresponding phase portrait map

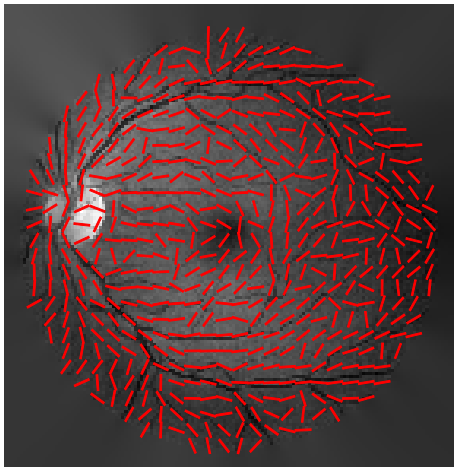

Orientation field

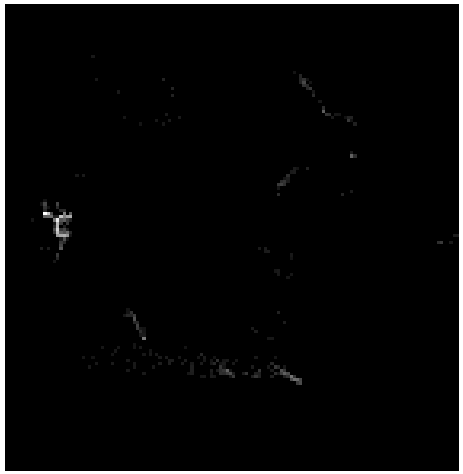

Log (1+Node)
[0, 1.526]

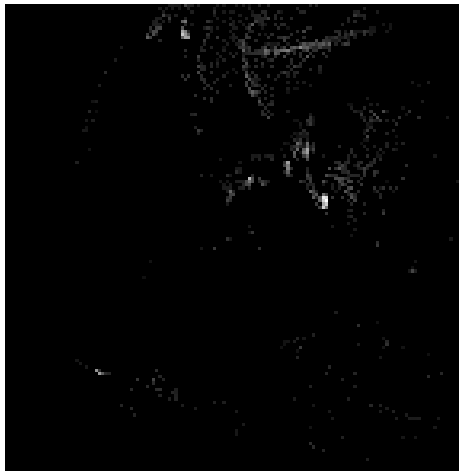

Log (1+Saddle)
[0, 1.576]

A: real eigenvalues of same sign

UNIVERSITY OF CALGARY

Results of Detection of the Center of the ONH

DRIVE Image 01

Magnitude response of the Gabor filters

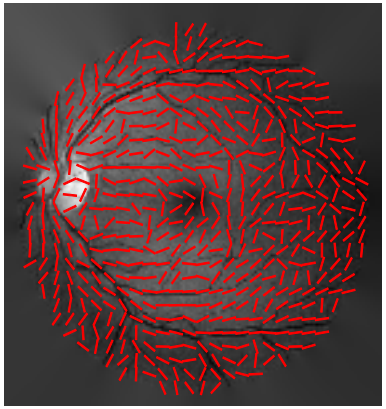

Orientation field

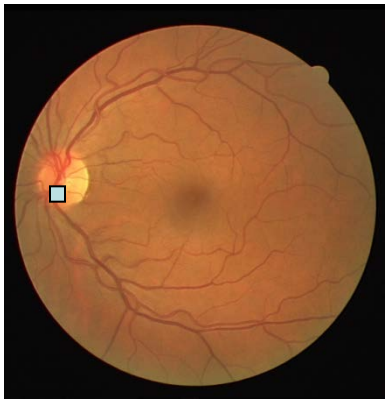

Successfully detected center of ONH

Results of Detection of the Center of the ONH

Statistics for the 40 images in the DRIVE database

Method	Distance mm (pixels)	
	mean	std
First peak in node map	1.61 (80.7)	2.40 (120)
Peak selected using intensity condition	0.46 (23.2)	0.21 (10.4)

Average ONH width (ONHW) for adults = 1.6 mm

UNIVERSITY OF CALGARY

Measurement of Retinal Vascular Thickness

- Retinal vascular changes can be indicative of diabetic retinopathy, RoP, and hypertension
- The width of the MTA increases in the presence of the diseases mentioned above
- Small changes are hard to detect by the naked eye, especially in the case of RoP

UNIVERSITY OF CALGARY

Processing Steps to obtain Vessel Skeleton

- GMR normalized and divided into superior and inferior parts using the center of the ONH
- Superior/inferior parts enhanced using gamma correction, binarized, and cleaned with “area open”
- ONH area and its boundary removed
- Branching points on each skeleton identified and removed
- Each skeleton segment labeled with a number

UNIVERSITY OF CALGARY

Tracking the MTA

- Seed label selected as the label with the highest average GMR in an annular region around the ONH
- Neighboring label to the previously selected label with the highest average GMR selected as the next segment
- Previous step repeated until no more labels are left

UNIVERSITY OF CALGARY

Interpolation of Vessel Edges

- The median absolute deviation of the Gabor angle responses of the selected MTA labels used to obtain linear segments
- Canny's method used to obtain edge-pixel candidates for each linear segment
- Vessel edges interpolated as two first-order polynomials fitted to the edge-pixel candidates on either side of a linear segment

UNIVERSITY OF CALGARY

MTA Width Measurement

- The normal line at each MTA skeleton pixel obtained using the Gabor-angle response
- The point of intersection between the normal line and the two edge lines obtained
- MTA width at a given pixel computed as the Euclidean distance between the two points of intersection

UNIVERSITY OF CALGARY

Vessel Width Measurement: No Plus Disease

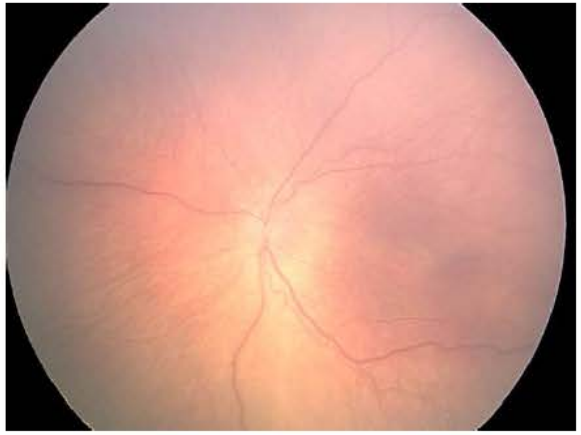

(a)

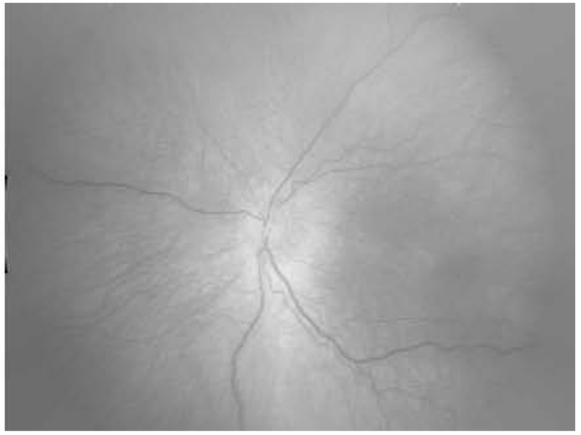

(b)

(c)

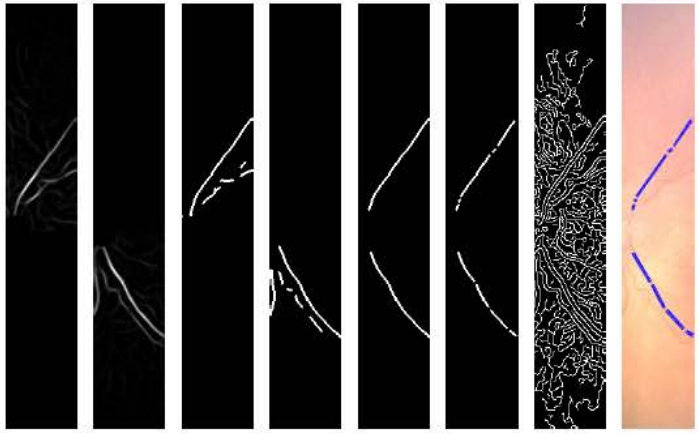

(d) (e) (f) (g) (h) (i) (j) (k)

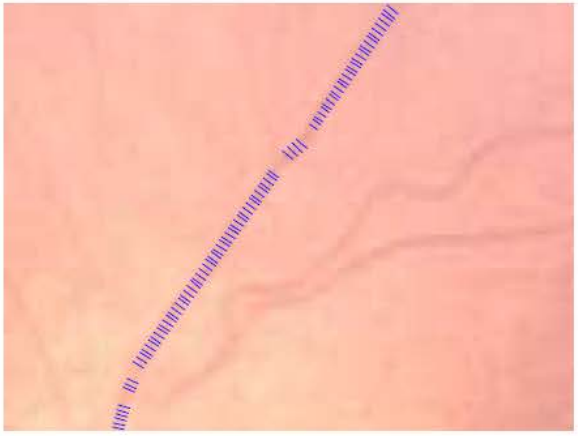

(l)

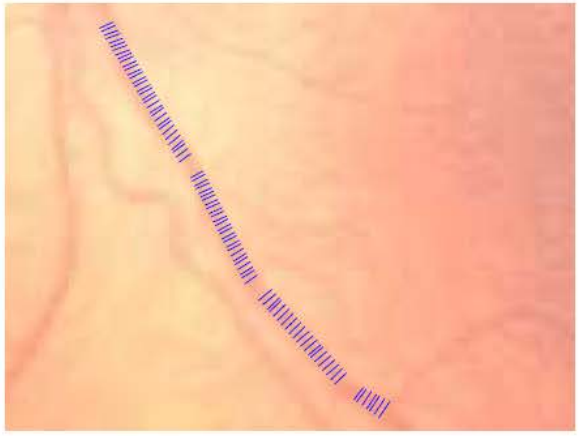

(m)

UNIVERSITY OF CALGARY

Vessel Width Measurement: Plus Disease

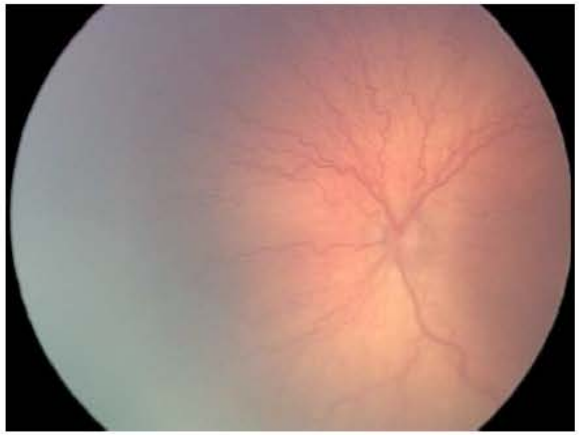

(a)

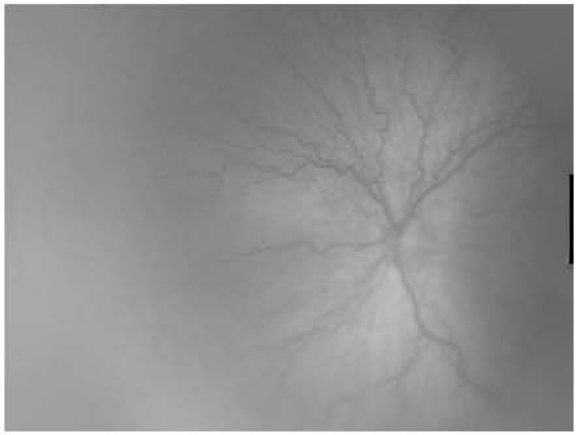

(b)

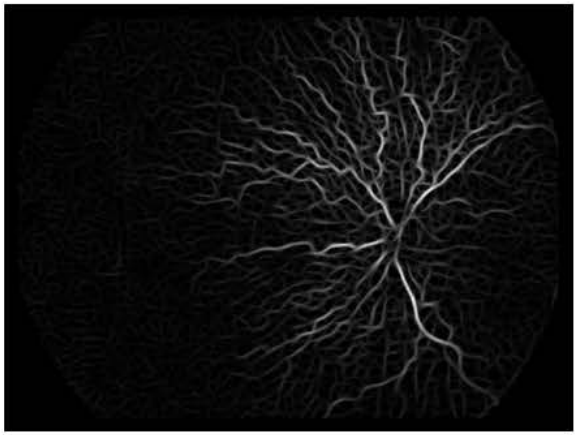

(c)

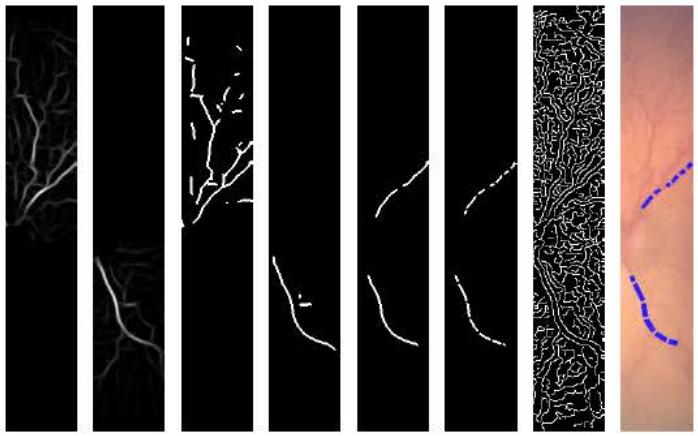

(d) (e) (f) (g) (h) (i) (j) (k)

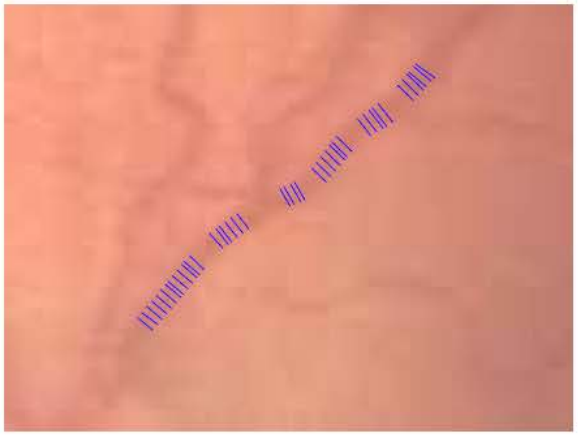

(l)

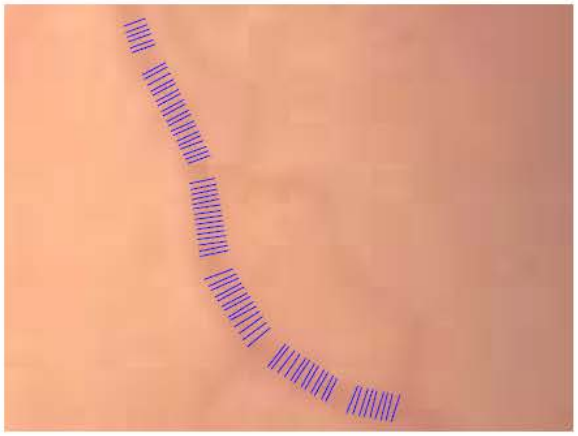

(m)

MTA Width: Results for Plus Disease

	MTA Width μm		
Class	**Mean ± STD**	**Minimum**	**Maximum**
No Plus ($n = 91$)	110.6 ± 18.5	83.0	180.8
Plus ($n = 19$)	125.0 ± 17.3	96.7	161.2

The results indicate a statistically highly significant difference between the means of the MTA width between the two classes (p = 0.002) and good diagnostic accuracy with A_z = 0.76

UNIVERSITY OF CALGARY

MTA Width: Results for Stages of RoP

	S1 $(n = 30)$	**S**2 $(n = 23)$	**S**3 $(n = 8)$
S0 $(n = 30)$	0.603	0.397	0.009^{**}
S1 $(n = 30)$	–	0.641	0.004^{**}
S2 $(n = 23)$	–	–	0.007^{**}

The results (p-values) indicate statistically highly significant differences between the means of the MTA width between Stage 3 and Stages 0, 1, and 2

UNIVERSITY OF CALGARY

GUI for Detection and Modeling of the MTA

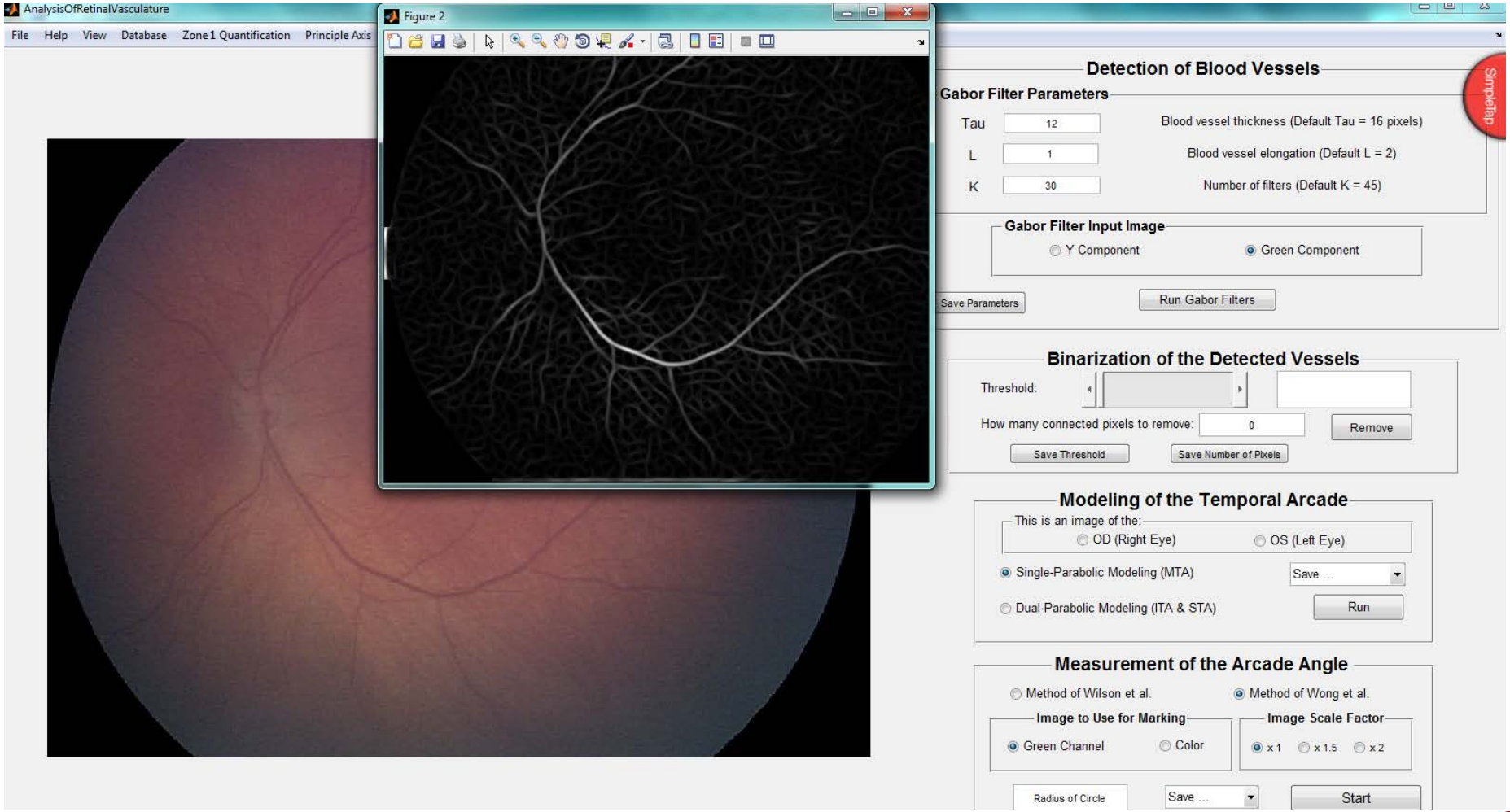

UNIVERSITY OF CALGARY

Derivation of the Vessel Map

- GMR with a large value for thickness ($\tau = 16$) used to emphasize the MTA ($l = 2$)
- GMR binarized using a fixed threshold
- Binary image skeletonized
- Skeleton image cleaned using the morphological area open procedure

Original

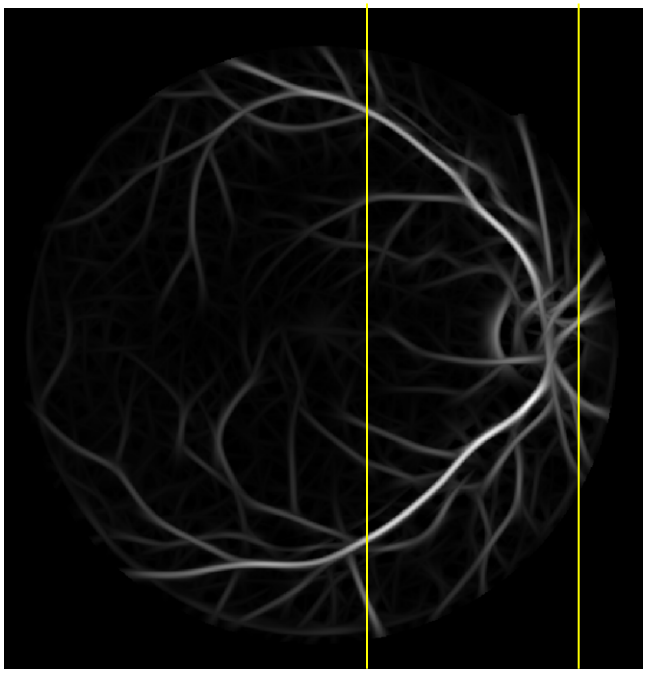

Vessel Map

Skeleton

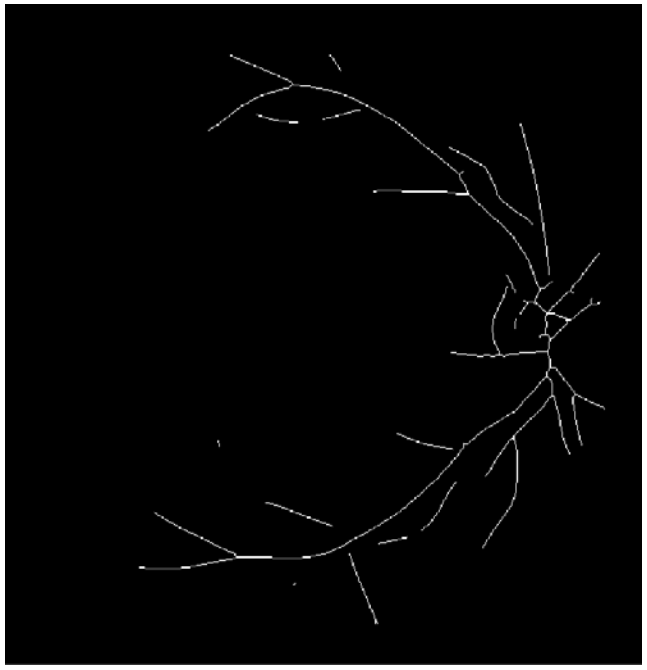

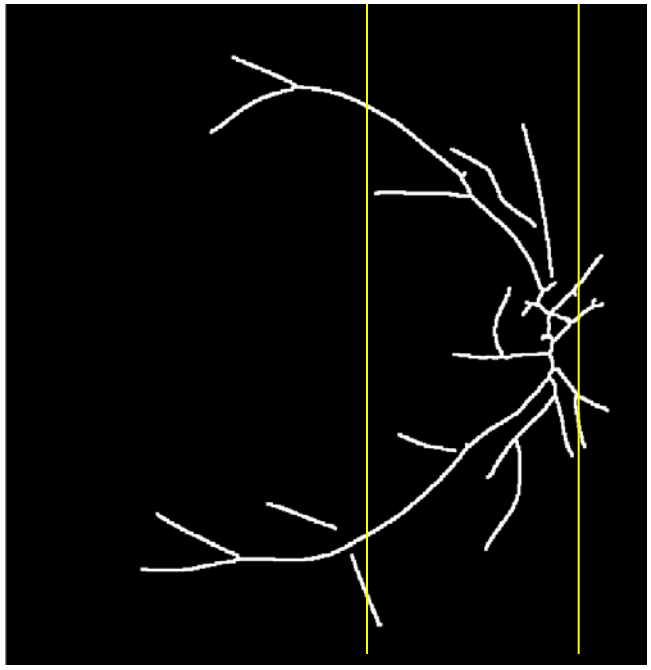

Cleaned Skeleton

UNIVERSITY OF CALGARY

The GHT for Parabolic Modeling

The GHT is a flexible method for parametric detection of curves such as parabolas

The general formula to define a parabola is

$$(y - y_o)^2 = 4\,a\,(x - x_o)$$

where (x_o, y_o) is the vertex

and a is the openness parameter

UNIVERSITY OF CALGARY

The GHT for Parabolic Modeling

- The parameters (x_o, y_o, a) define the 3D Hough space, represented by an accumulator A
- For every nonzero pixel in the image domain, there exists a parabola in the Hough space for each value of a
- A single point in the Hough space defines a parabola in the image domain

UNIVERSITY OF CALGARY

Anatomical Restrictions on the Hough Space

- The MTA follows a parabolic path up to the macula only
- Given that the macula is about 2×ONHW temporal to the ONH and prior knowledge of the ONH, we restrict the horizontal size of the Hough space
- Size of each plane is 584 x 170 pixels for DRIVE images

UNIVERSITY OF CALGARY

Anatomical Restrictions on the Hough Space

- The location of the vertex of the desired parabola in the Hough space is restricted to be within 0.25×ONHW of the ONH center
- The value of a has a physiological limit: in the range [35, 120] for DRIVE
- The number of planes in the 3D Hough space is 86

Hough space updated with Gabor Mag. with vertex and horizontal size restrictions

Hough space updated with Gabor Mag. with horizontal size restriction

Hough space updated with unity with vertex and horizontal size restrictions

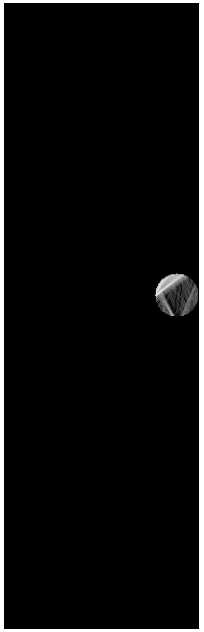

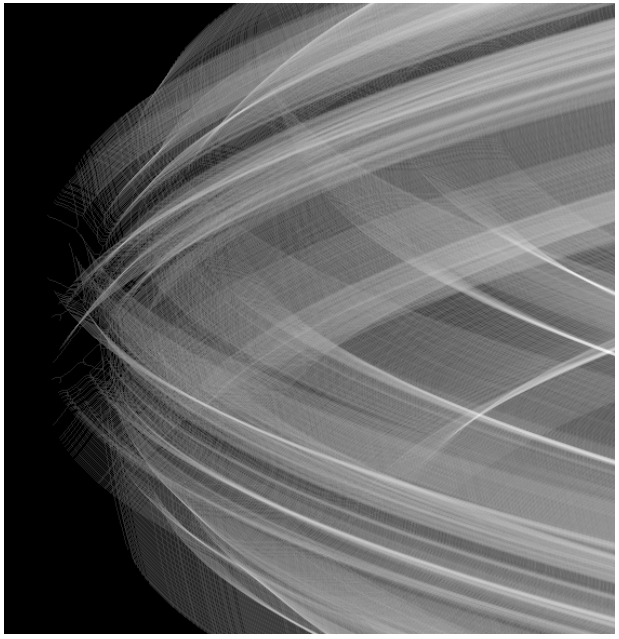

Hough space updated with unity

UNIVERSITY OF CALGARY

Dual-parabolic Modeling

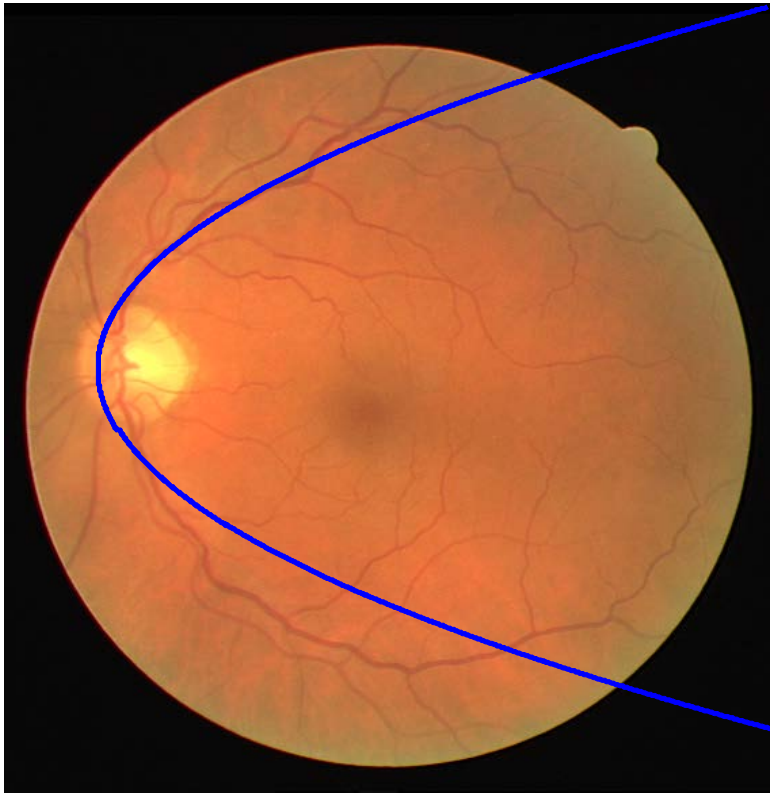

Parabolic fit using Gabor-magnitude-updated GHT

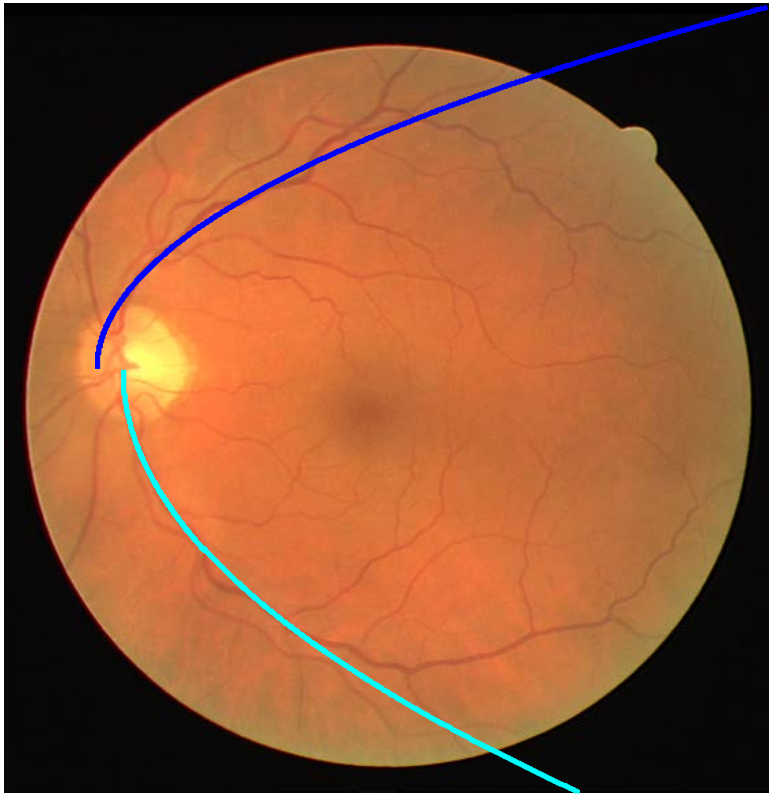

Dual-parabolic fit using Gabor-magnitude-updated GHT

UNIVERSITY OF CALGARY

Results: Single- and Dual-parabolic Models

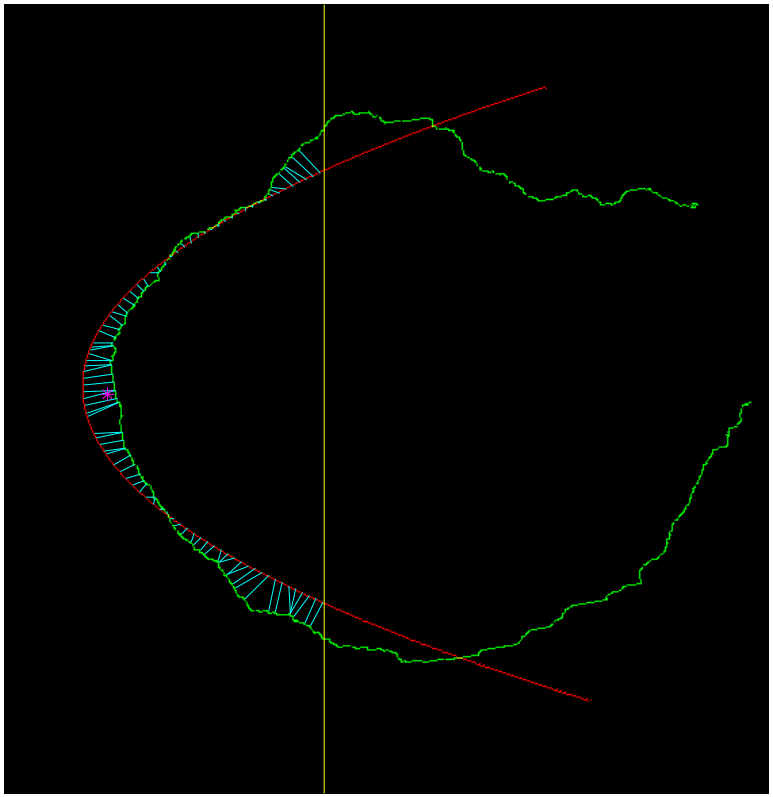

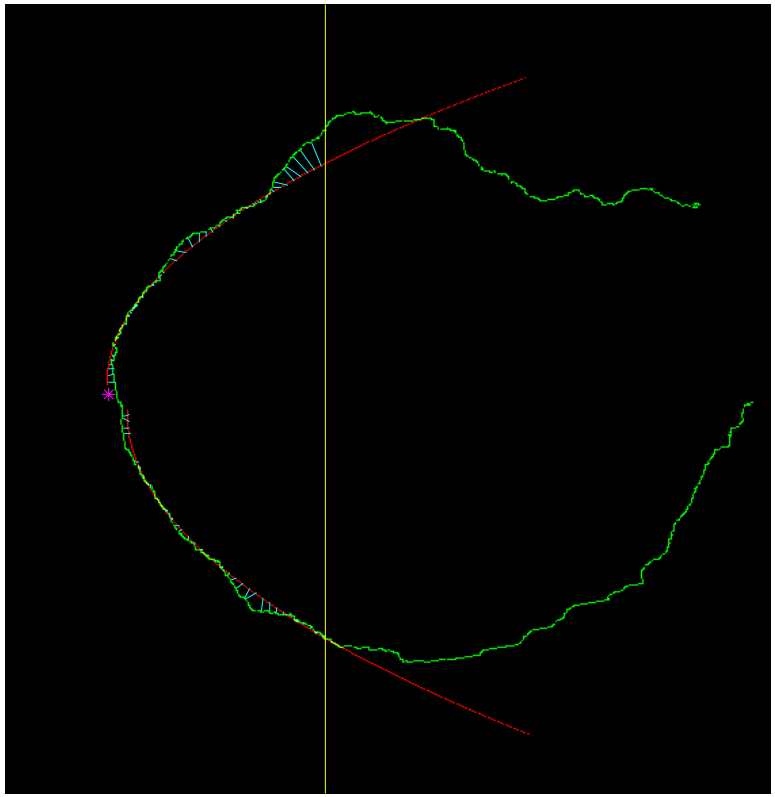

Single model: MDCP = 11.5 pixels

Dual model: MDCP = 3.11 pixels

MDCP = mean distance to closest point

UNIVERSITY OF CALGARY

Measurement of the Arcade Angle

- TAA measured via graphical user interface (GUI)
- User prompted to mark the center of the ONH
- Circle with given radius drawn on the image
- User prompted to mark the points of intersection of the circle with the superior and inferior venules
- TAA measured as the angle between the three manually marked points

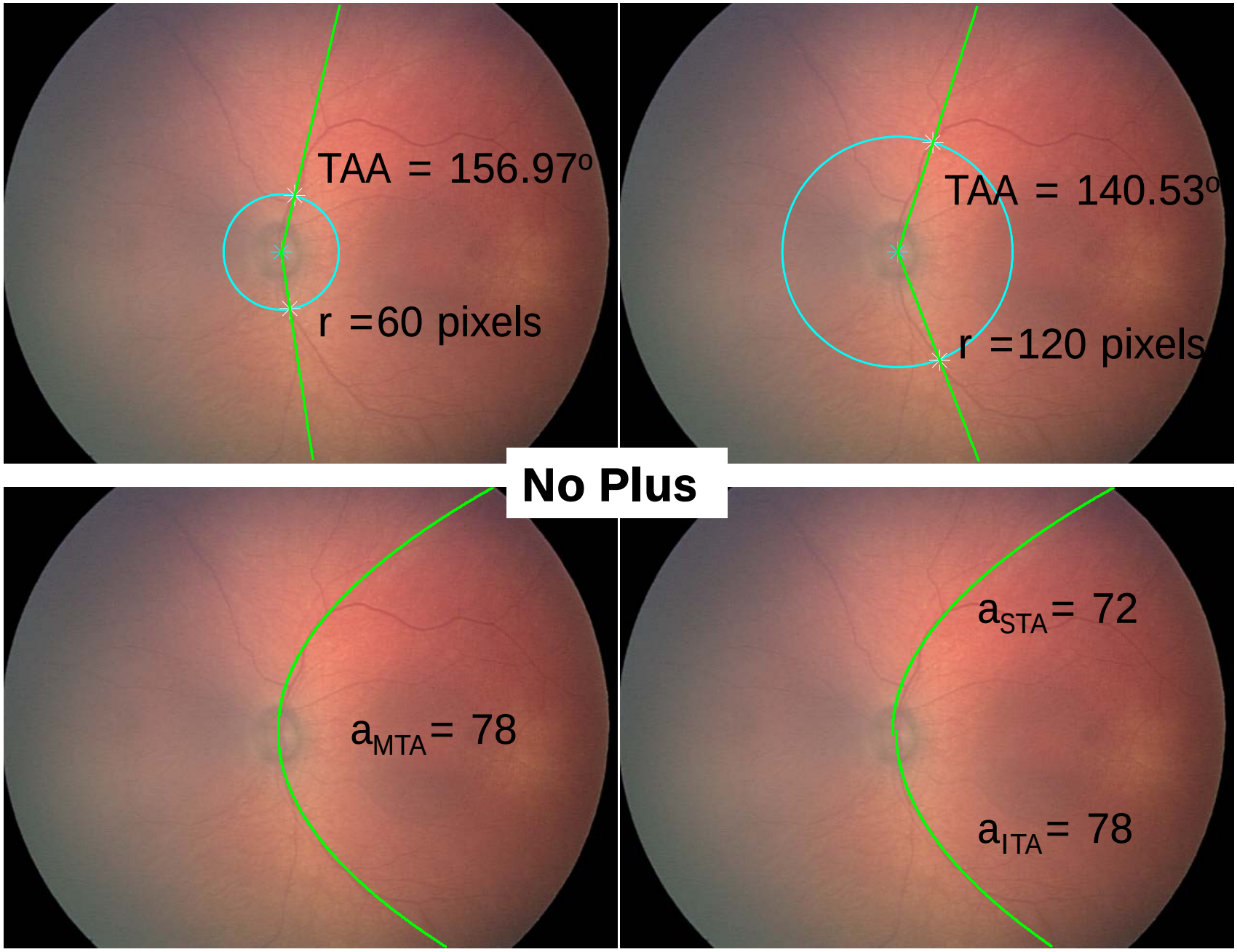
TAA = 156.97°
r =60 pixels
TAA = 140.53°
r =120 pixels
No Plus
a_{MTA}= 78
a_{STA}= 72
a_{ITA}= 78

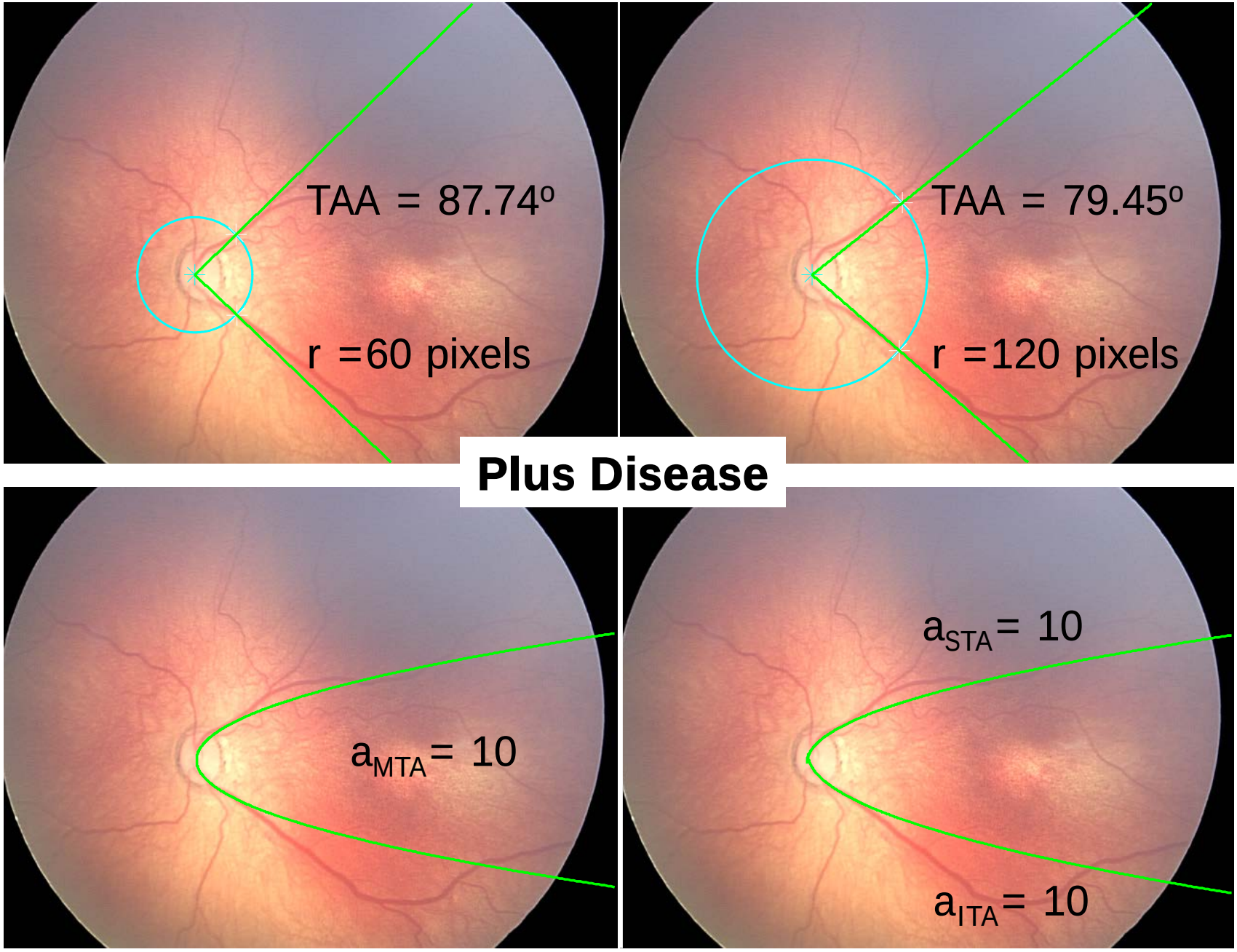
TAA = 87.74°
r =60 pixels
TAA = 79.45°
r =120 pixels
Plus Disease
a_{MTA}= 10
a_{STA}= 10
a_{ITA}= 10

UNIVERSITY OF CALGARY

MTA Openness: Results

Parameter	Mean A_z (SE)	CI_s $\alpha = 0.025$	Statistical Significance
TAA, $r = 60$	0.74 (0.0076)	[0.721, 0.752]	$18^{**}, 19^{*}$
TAA, $r = 120$	0.69 (0.0101)	[0.672, 0.712]	$12^{**}, 15^{*}$
$\lvert a_{\mathrm{MTA}} \rvert$	0.70 (0.0102)	[0.683, 0.724]	$0^{**}, 0^{*}$
$\lvert a_{\mathrm{STA}} \rvert$	0.71 (0.0100)	[0.687, 0.727]	$4^{**}, 15^{*}$
$\lvert a_{\mathrm{ITA}} \rvert$	0.67 (0.0086)	[0.651, 0.685]	$0^{**}, 0^{*}$

19 cases with plus disease compared with
19 randomly selected no-plus cases, repeated 50 times

UNIVERSITY OF CALGARY

Results: Proliferative Diabetic Retinopathy (PDR)

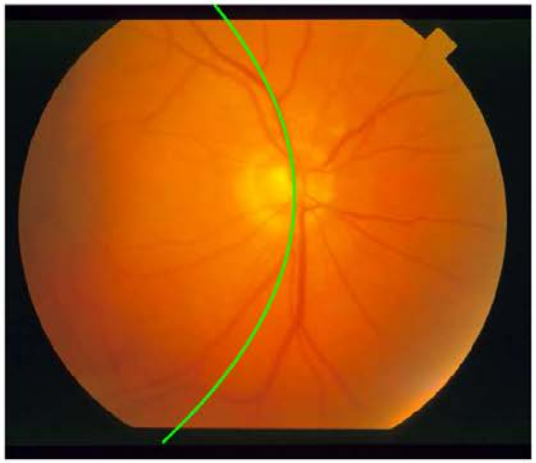

Normal: aMTA = -153

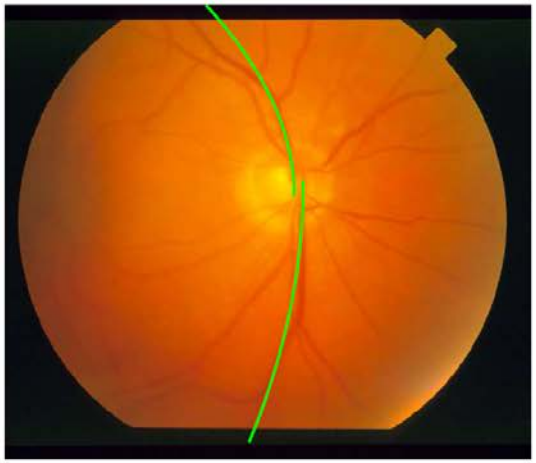

aSTA = -138, aITA = -420

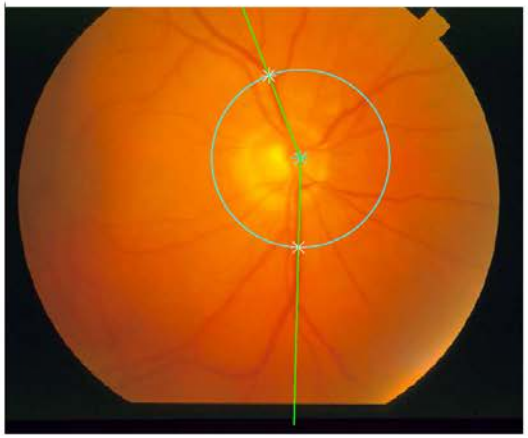

TAA = 157.8°

PDR: aMTA = 55

aSTA = 36, aITA = 48

TAA = 110.4°

UNIVERSITY OF CALGARY

PDR: ROC Analysis

Parameter	Normal ($n = 11$) Mean $\pm$ STD	PDR ($n = 11$) Mean $\pm$ STD	A_z (SE)	p-value
Arcade Angle (Degrees)	151.00 ± 11.23	139.01 ± 11.96	0.80 (0.093)	0.0156
$\lvert a_{\mathrm{MTA}} \rvert$	140.40 ± 61.35	86.27 ± 26.76	0.87 (0.096)	0.0026
$\lvert a_{\mathrm{STA}} \rvert$	84.93 ± 27.66	88.36 ± 46.28	0.49 (0.122)	0.7839
$\lvert a_{\mathrm{ITA}} \rvert$	166.80 ± 98.72	89.18 ± 51.43	0.82 (0.088)	0.0164

UNIVERSITY OF CALGARY

Openness of MTA: Discussion

- First study to quantify the effects of plus disease on the openness of the MTA
- Diagnostic performance (A_z) of the parameters of the parabolic models is comparable to that provided by TAA
- The measures show a decrease in the openness of the MTA in the presence of plus disease

UNIVERSITY OF CALGARY

Measurement of Retinal Vascular Tortuosity

- The tortuosity of vessels increases in the presence of plus disease
- Tortuosity does not have a formal definition: its quantification needs to take into account the clinical relevance of the measure
- Tortuosity measures in the literature either do not consider the orientation of vessels or obtain it using skeleton pixels: prone to error

UNIVERSITY OF CALGARY

Processing Steps to Obtain Vessel Skeleton

- GMR binarized and cleaned with “area open”
- Binary image skeletonized, spurs of length up to 5 pixels removed
- Branching points on the skeleton identified and removed
- Each skeleton segment labeled with a number
- Linear parts identified and removed using the median absolute deviation of Gabor angles

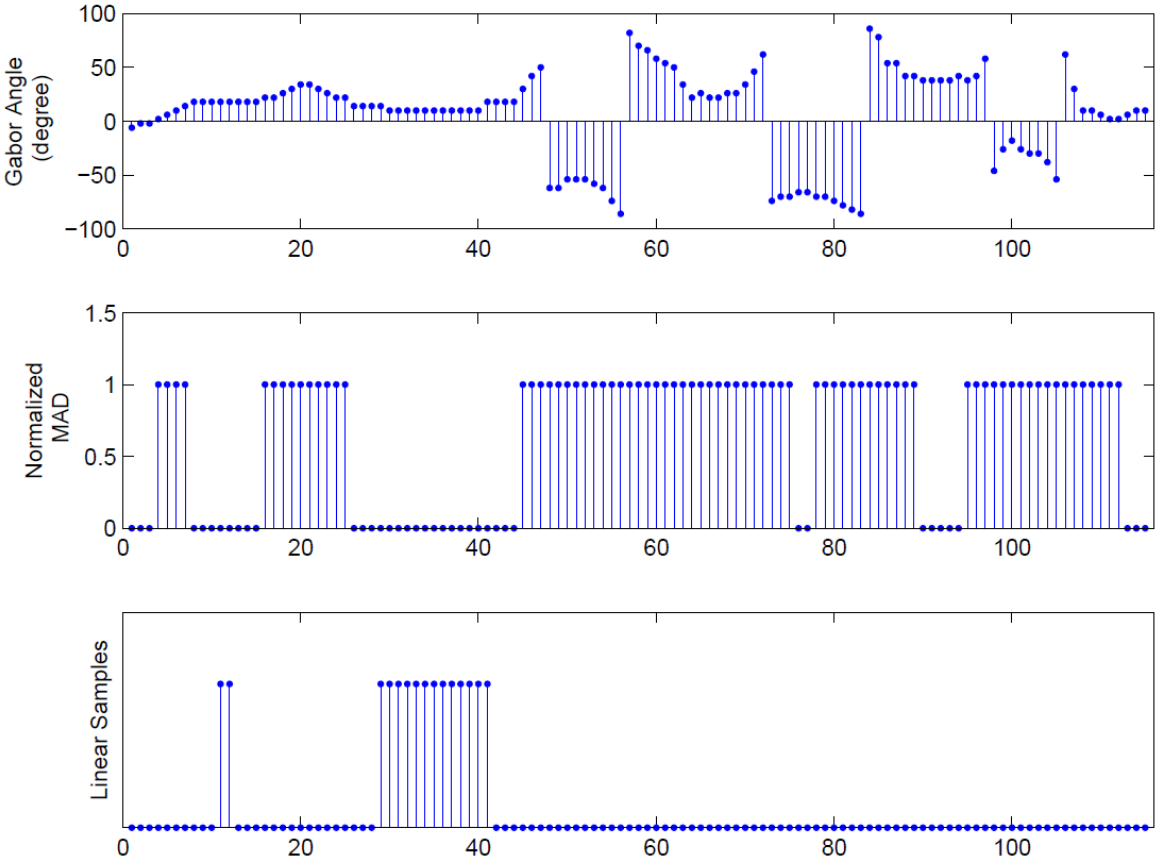
Gabor Angle (degree)
100
50
0
−50
−100
0
20
40
60
80
100
Normalized MAD
1.5
1
0.5
0
0
20
40
60
80
100
Linear Samples
0
20
40
60
80
100

(a)

(b)

(c)

(d)

UNIVERSITY OF CALGARY

Angle-Variation-Based Tortuosity Measure

- Angle-variation index (AVI) based on the Gabor angle at a given pixel:

$$\mathrm{AVI}(p) = \frac{1}{2}\left\{\left|\sin\left[\phi(p) - \phi(p-1)\right]\right| + \left|\sin\left[\phi(p) - \phi(p+1)\right]\right|\right\}$$

- Average AVI for a vessel segment:

$$\mathrm{AVT} = \frac{1}{N}\sum_{n=1}^{N}\mathrm{AVI}(n)$$

- AVT normalized to [0, 1] for each segment

UNIVERSITY OF CALGARY

Examples of the AVT Measure

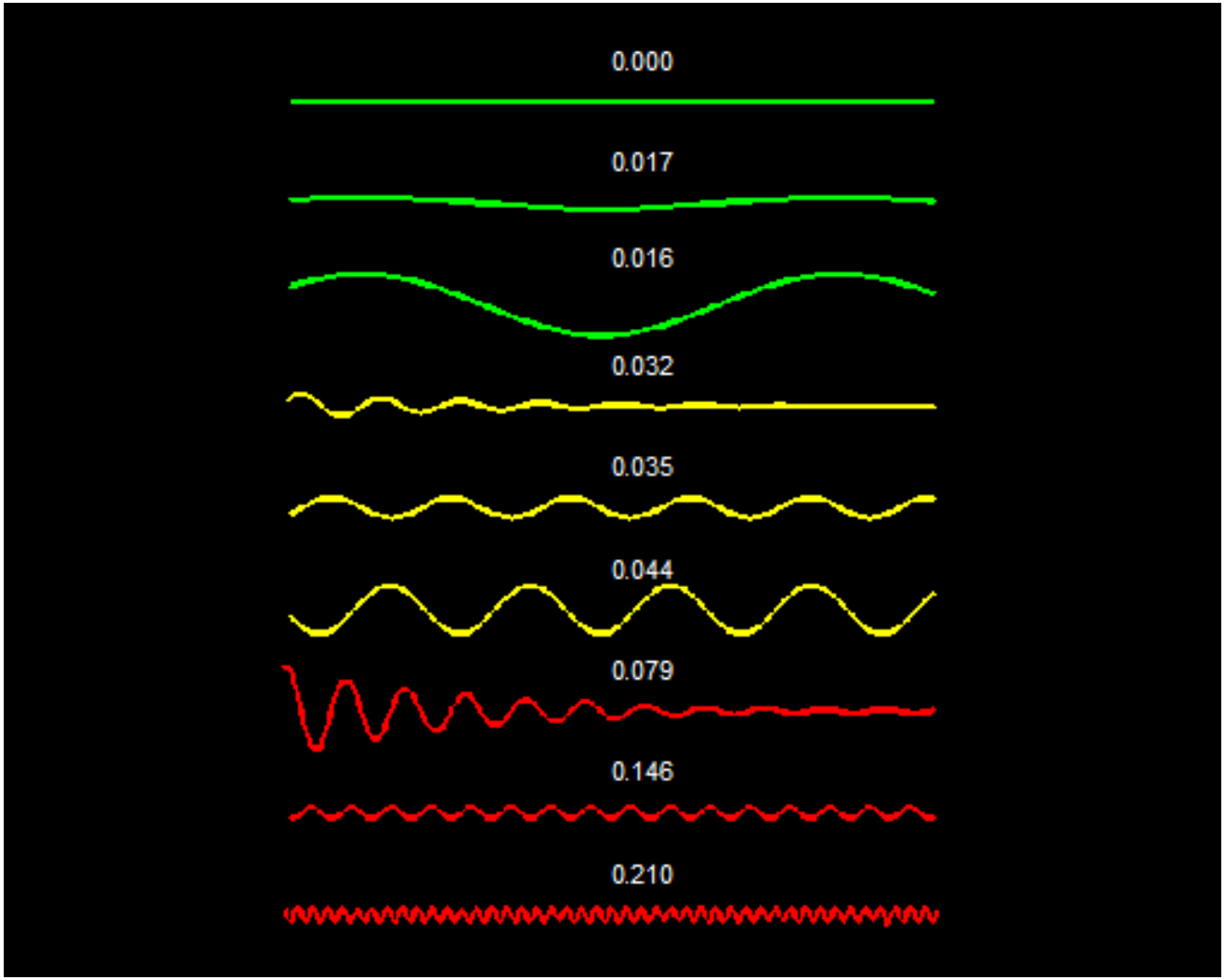

UNIVERSITY OF CALGARY

Diagnostic Decision-Making Criterion

- Independent training set used to obtain AVT threshold to detect tortuous vessels
- Minimum tortuous vessel length threshold determined using the training set
- Plus disease diagnosed if at least 5 mm of tortuous vessels present in one quadrant or 2.5 mm present in each of two quadrants

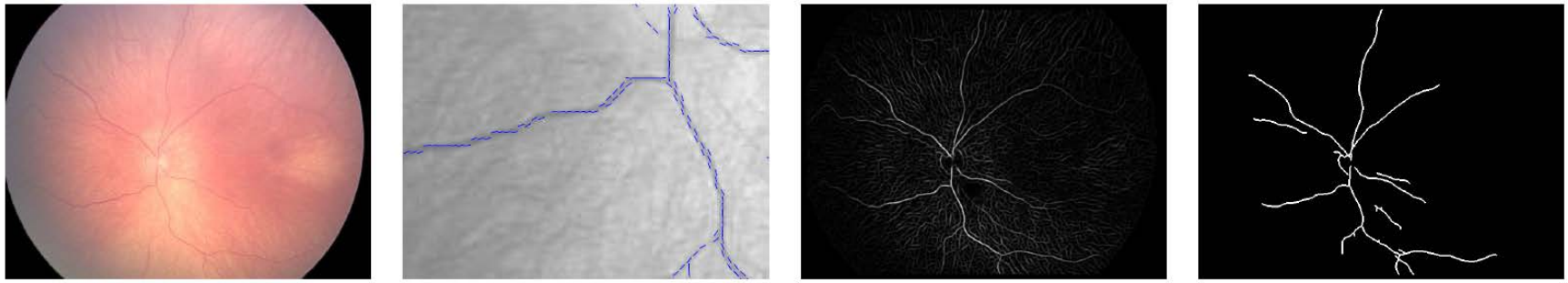

Case with no plus disease: 0 mm of tortuous vessels

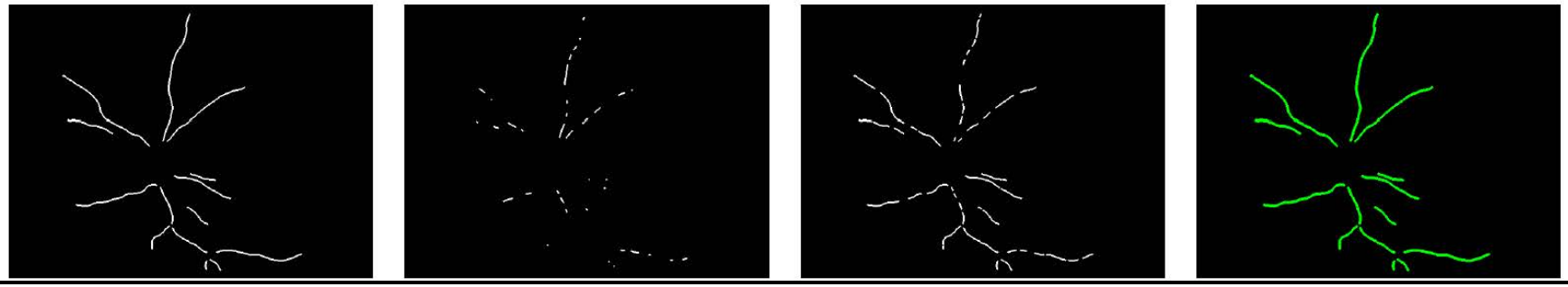

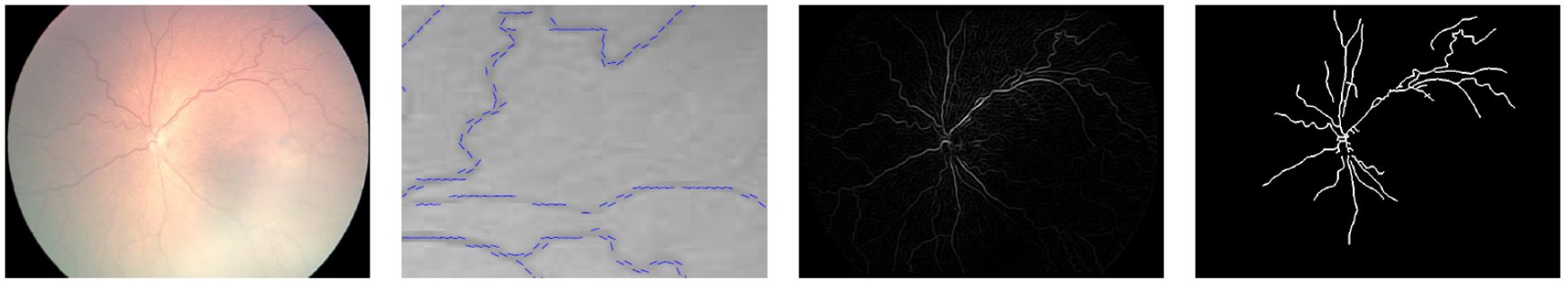

Case with plus disease: 11.75, 4.20, 1.99, and 1.42 mm in the four quadrants

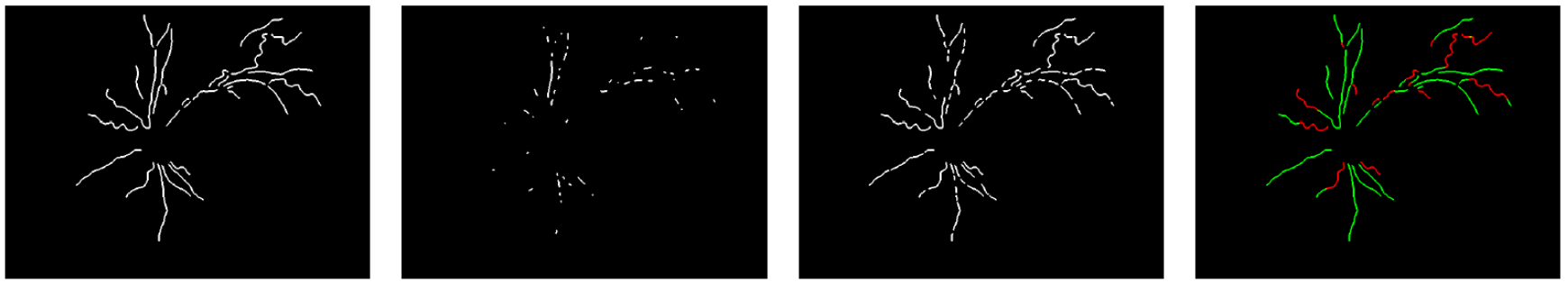

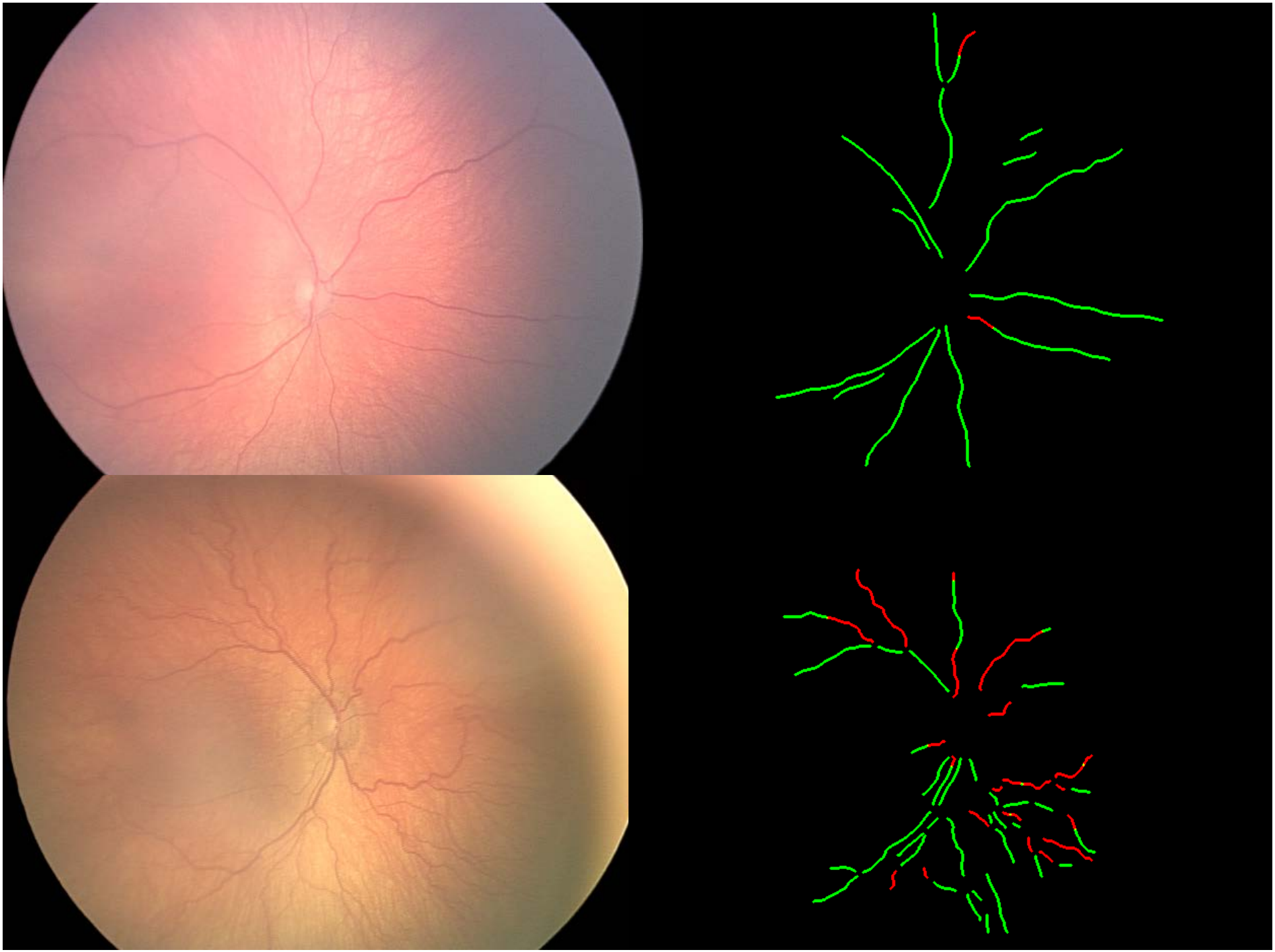

UNIVERSITY OF CALGARY

Application of AVT to Diagnose Plus Disease

- The proposed AVT measure and the diagnostic decision-making criterion applied to 91 images without plus and 19 with plus
  - Sensitivity = 0.89 (17/19)
  - Specificity = 0.99 (90/91)
- Results indicate high sensitivity and excellent specificity in diagnosis of plus disease with area under the ROC curve up to 0.98

UNIVERSITY OF CALGARY

Tortuosity: Discussion

- All studies available in the literature on diagnosis of plus disease based on vessel tortuosity require manual marking and/or selection of vessels to be analyzed

- Our vessel detection methods are fully automated and capable of distinguishing all tortuous vessels in a given image without any manual selection and/or correction

UNIVERSITY OF CALGARY

Conclusion

- Digital image processing techniques can assist in quantitative analysis of retinal vasculature
- Pattern recognition techniques can facilitate CAD of RoP
- CAD of RoP can assist in improved diagnosis, analysis of the effects of treatment, and clinical management of RoP

UNIVERSITY OF CALGARY

Thank You!

- This work was supported by the Natural Sciences and Engineering Research Council of Canada
- We thank Paola Casti for her contributions to the design of the MTA tracking algorithm, Eliana Almeida for suggesting the MAD measure, and April Ingram for help with the TROPIC database

http://people.ucalgary.ca/~ranga/